Behavioral/Systems/Cognitive

Intrinsic and Functional Differences among Commissural Interneurons during Fictive Locomotion and Serotonergic Modulation in the Neonatal Mouse

Guisheng Zhong, Manuel Díaz-Ríos, and Ronald M. Harris-Warrick
Department of Neurobiology and Behavior, Cornell University, Ithaca, New York 14853

Commissural interneurons (CINs) send their axons across the midline to innervate contralateral targets and have been implicated in the coordination of left–right limb movements during locomotion. In the neonatal mouse spinal cord, we studied the firing properties and responses to serotonin (5-HT) of two classes of CINs: those whose axons turn caudally after crossing the midline (dCINs) and those whose axons bifurcate after crossing the midline (adCINs). During NMDA and 5-HT-induced locomotor-like activity, a majority of lumbar (L2) dCINs fired rhythmically with ventral root-recorded motor activity, although their firing phase was widely distributed throughout the locomotor cycle. In contrast, none of the adCINs fired rhythmically during fictive locomotion. We studied the baseline firing and membrane properties, and responses to current injection, in dCINs and adCINs that had been partially isolated by blockade of rapid synaptic transmission (with antagonists to glutamate, GABA, and glycine). No significant baseline differences were found between the cell types. In contrast, 5-HT significantly increased the excitability of the isolated dCINs by depolarizing the membrane potential, reducing the postspike afterhyperpolarization amplitude and decreasing the action potential threshold. None of these parameters were affected by 5-HT in adCINs. These results, together with our recent study of a third class of CINs, the aCINs whose axons ascend after crossing the midline (Zhong et al., 2006), suggest that dCINs and aCINs, but not adCINs, are excited by 5-HT and are rhythmically active during fictive locomotion. Thus, they may play important roles in the coordination of left–right movements during fictive locomotion.

Key words: **mouse; spinal cord; locomotion; commissural interneuron; serotonin; NMDA**

Introduction

Commissural interneurons (CINs), which send their axons across the midline in the spinal cord, are believed to play a critical role in left–right coordination during locomotion in rodents (Butt et al., 2002; Butt and Kiehn, 2003; Lanuza et al., 2004). Spinal CINs have been anatomically classified into four different types in rats and mice (Eide et al., 1999; Stokke et al., 2002; Nissen et al., 2005) based on the direction of their axonal projections: ascending (aCIN, axons travel rostrally after crossing the midline), descending (dCIN, axons travel caudally), bifurcating (adCIN, axons bifurcate after crossing the midline and travel both rostrally and caudally), and short-range intrasegmental (axons remain locally within 1.5 segments of their somata) CINs. CINs make inhibitory or excitatory synapses onto motoneurons and other interneurons on the opposite side of the spinal cord (Bannatyne et al., 2003; Birinyi et al., 2003; Butt and Kiehn, 2003; Lanuza et al., 2004; Quinlan and Kiehn, 2005). In the neonatal rat, dCINs have been demonstrated to be involved in left–right alternation during fictive locomotion (Butt et al., 2002; Butt and Kiehn, 2003). The firing patterns of the dCINs were not homogeneous during NMDA and serotonin (5-HT)-induced locomotor-like activity, ranging from highly rhythmic bursting to dCINs that remained silent and did not participate in the motor pattern (Butt et al., 2002). However, in these previous studies, the "dCIN" pool analyzed included an unknown number of adCINs, and thus it is not yet clear whether these two anatomically distinct CIN populations have different roles in fictive locomotion.

In this study, we used the neonatal mouse spinal cord to characterize the cellular firing properties of identified dCINs and adCINs during fictive locomotion evoked by the application of NMDA and 5-HT (Cazalets et al., 1992, 1995; Kjaerulff and Kiehn 1996; Branchereau et al., 2000). CINs were monitored with whole-cell patch recordings from the L2 spinal segment, and their activity correlated to rhythmic flexor motor activity measured by extracellular recordings from the L2 ventral roots. 5-HT is thought to play an important role to organize the locomotor network for rhythmic activity (MacLean et al., 1998; Madriaga et al., 2004; Christie and Whelan, 2005; Liu and Jordan, 2005; Pearlstein et al., 2005), so we also studied the modulatory effects of 5-HT on the intrinsic membrane properties of dCINs and adCINs that were pharmacologically isolated from most fast synaptic inputs. Our results indicate that, in the mouse, a majority of dCINs fire rhythmically, whereas none of the adCINs show rhythmicity during fictive locomotion. Furthermore, 5-HT de-

Received Jan. 13, 2006; revised May 3, 2006; accepted May 3, 2006.

This work was supported by National Institutes of Health Grants R01-NS35631 (R.M.H.-W.) and R01-NS050943 (J. Guckenheimer). We thank Dr. Bruce Johnson and Marie Goeritz for helpful comments on this manuscript.

Correspondence should be addressed to Dr. Ronald M. Harris-Warrick, Department of Neurobiology and Behavior, Cornell University, W159 Seeley G. Mudd Hall, Ithaca, NY 14853. E-mail: rmh4@cornell.edu.

DOI:10.1523/JNEUROSCI.1410-06.2006

 0270-6474/06/266509-09$15.00/0

polarizes and increases the excitability of dCINs but has no effect on adCINs. In a previous study (Zhong et al., 2006), we showed that aCINs also fire rhythmically during fictive locomotion and are excited by 5-HT. Our results suggest that these anatomically distinct CINs can be functionally differentiated: dCINs and aCINs, but not adCINs, are potential components of the spinal locomotor network of the neonatal mouse.

Materials and Methods

Whole-cord preparations. Experiments were performed using spinal cords of postnatal day 0 (P0) to P4 ICR mice (Taconic Farms, Hudson, NY). The animal protocol was approved by the Animal Use and Care Committee at Cornell University and was in accordance with National Institutes of Health guidelines. Animals were killed by decapitation, and their spinal cords from segment C5 to S3 were ventrally dissected and isolated under ice-cold (4°C) oxygenated (95% O_2/5% CO_2) low-calcium Ringer's solution (in mM: 128 NaCl, 4.7 KCl, 1.2 KH_2PO_4, 0.25 $CaCl_2$, 1.3 $MgCl_2$, 3.25 $MgSO_4$, 25 $NaHCO_3$, and 22 D-glucose). The spinal cord was pinned ventral side up and superfused with oxygenated normal Ringer's solution (in mM: 111 NaCl, 3.08 KCl, 25 $NaHCO_3$, 1.18 KH_2PO_4, 1.25 $MgSO_4$, 2.52 $CaCl_2$, and 11 D-glucose) for 1 h at room temperature (20–22°C) before starting the experiment.

To make whole-cell recordings from the intact cord, a patch electrode pulled from thick-walled borosilicate glass (World Precision Instruments, Sarasota, FL) on a vertical puller (Narishige, Tokyo, Japan) with resistances of 6–8 MΩ was lowered into a small slit in the ventromedial surface of the L2 segment. The pipette solution contained the following (in mM): 138 K-gluconate, 10 HEPES, 5 ATP-Mg, 0.3 GTP-Li, and 0.0001 $CaCl_2$, pH 7.4 with KOH. The seal resistance obtained before recordings was always >1 GΩ. Blind patch-clamp recordings were made with a Multiclamp 700A amplifier (Molecular Devices, Palo Alto, CA) and were driven by Clampex (pClamp 9; Molecular Devices). Under our experimental conditions, the liquid junction potential of the electrode was ~8 mV (with the cell more hyperpolarized than the pipette voltage) and was corrected off-line. Data were filtered at 2–10 kHz and digitized at 10 or 20 kHz. The shape of the action potential was unaffected by the filtering.

To identify the CINs, the hemicord was slit along the midline rostrally between T13 and L1 and caudally between L4 and L5 for several segments before performing a contralateral transverse hemisection and extending the section midsagittally, thus liberating short lengths of contralateral hemicords several segments rostral and caudal of the recording site (Fig. 1*A*). These contralateral rostral and caudal hemicords were gently sucked into stimulation electrodes (Fig. 1*A*). Brief current pulses (50–300 μA) were delivered to stimulate axons that were contralateral and rostral or caudal to the recorded neuron. Commissural interneurons were identified by a collision test (Fig. 1*C*), in which orthodromic action potentials evoked by current injection in the soma collided with and eliminated appropriately timed antidromic action potentials evoked by stimulation of the contralateral hemicord (Zhong et al., 2006). Cells were accepted as CINs if they passed a collision test with hemicord stimulation with glutamatergic, GABAergic, and glycinergic fast synaptic transmission blocked.

Locomotor-like activity was evoked by bath superfusion with Ringer's solution containing a combination of NMDA (3–10 μM) and 5-HT (6–15 μM). Recordings were made by placing suction electrodes on one to three ventral roots [contralateral L2 (cL2) in all experiments; ipsilateral L2 (iL2) and iL5 in many experiments (Fig. 1*B*)] to characterize NMDA/5-HT-induced locomotor-like activity. When patch-clamp recordings were made, one (cL2) or two (iL2 and cL2) (see Fig. 2*A*,*D*) ventral root recordings were included. A total of 100% of 31 experiments made with combined iL2–cL2 or iL2–cL2–iL5 recordings showed the expected alternation between ipsilateral and contralateral bursts and between flexor (L2) and extensor (L5) bursts during NMDA- and 5-HT-evoked fictive locomotion, suggesting that recordings made with a single ventral root reliably monitor rhythmic locomotor-like activity. Ventral root recordings were bandpass filtered (100 Hz to 1 kHz) and recorded using an alternating current amplifier (model 1600; A-M Systems, Carlsborg, WA). All drugs were purchased from Sigma (St. Louis, MO): D(−)-2-amino-5-phosphonopentanoic acid (AP-5), 6-cyano-7-nitroquinoxaline-2,3-dione disodium salt (CNQX), strychnine, picrotoxin, and tetrodotoxin.

Data analysis. Locomotor-like activity was recorded in the intact spinal cord preparation during bath application of NMDA and 5-HT. Clampfit 9.0 (Molecular Devices), Excel (Microsoft, Seattle, WA), and Spike 2 (Cambridge Electronic Design, Cambridge, UK) were used for data analysis. A cycle of motor nerve activity started at the onset of a contralateral L2 (cL2) ventral root burst and ended at the onset of the next cL2 burst; these onsets were determined by a custom-made program in Spike2 to detect when the rectified signal exceeded the average noise level between bursts by a preset amount. A double normalization process was used in this study to analyze the phasing of neural activity during the locomotor cycle (Shefchyk and Jordan, 1985; Berkowitz and Stein, 1994; Zhong et al., 2006). The period of cL2 activity was divided into the first five equal time bins, whereas the rest of the cycle (monitored with iL2

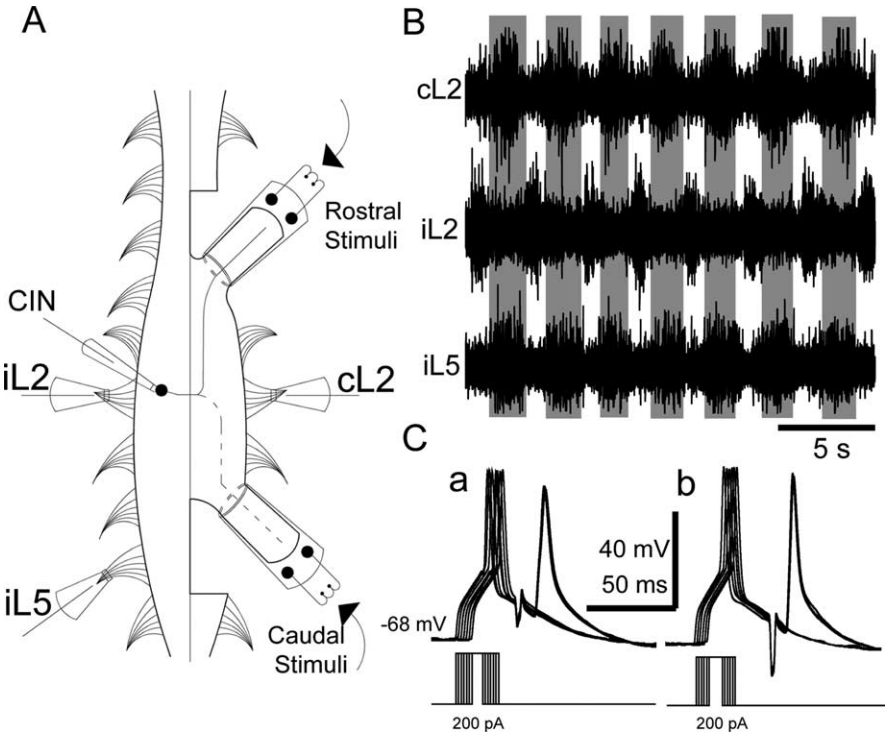

Figure 1. Experimental setup. ***A***, Stimulation suction electrodes were placed on the rostral and caudal contralateral hemicords at the level of T13–L1 and L4–L5, respectively, to stimulate the contralateral projecting axons of CINs. Additionally, three suction recording electrodes were placed to monitor nerve activities from iL2, cL2 (flexor nerves), and iL5 (extensor nerve). A patch-clamp electrode was inserted in a small slit made in the iL2 segment for neuronal recording. ***B***, Extracellular recordings from cL2, iL2, and iL5 ventral roots after application of 6 μM NMDA and 9 μM 5-HT, showing locomotor-like activity characterized by left–right and flexor–extensor alternation in a P2 spinal cord. The gray areas show the activity of ipsilateral extensor and contralateral flexor activity. ***C***, An example of a successful collision test from an adCIN. Six superimposed traces are shown in which the time between the orthodromic action potentials (first) and the antidromic action potential (second) is sequentially shortened. Antidromic action potentials caused by stimulating the rostral (***a***) or caudal (***b***) contralateral hemicord disappear in the last three traces. In both sets, fast glutamatergic, GABAergic, and glycinergic synaptic transmission was blocked pharmacologically.

recordings in many experiments) was divided into the second five equal time bins. The mean firing rate was established by dividing the number of action potentials in a bin by the duration for at least 35 cycles of activity. The average firing frequencies in each bin were used to create an activity histogram.

Circular statistics were used to determine the significance of the phasing of CIN firing during fictive locomotion (Kjaerulff and Kiehn, 1996; Zar, 2000). The latency to each spike was measured relative to the beginning of the cL2 ventral root burst. The mean latency was calculated as described by Kjaerulff and Kiehn (1996). The direction of a vector represents the average preferred phase of firing of the neuron, whereas its length, *r*, is a measure of statistical significance of the peak preferred phase, indicating the sharpness of the tuning of the spikes around their mean. Vectors with a phase in the range of 0.0–0.5 corresponded to cells firing in phase with cL2. *p* values for the significance of *r* were calculated as described by Kjaerulff and Kiehn (1996) and Zar (2000).

Firing properties of isolated CINs. dCINs and adCINs were isolated from most rapid synaptic inputs with a combination of AP-5 (15–20 μM) and CNQX (10 μM) to block glutamatergic synapses, picrotoxin (5 μM) to block GABAergic synapses, and strychnine (10 μM) to block glycinergic synapses. Some of the neurons fired spontaneously, whereas others were silent at rest and required depolarizing current pulses to evoke action potentials. To ensure uniformity of the measurements, all neurons were held below threshold at −68 mV with a bias current. Only neurons with action potentials with peak amplitudes above 0 mV were included in the analysis. To determine the *F–I* plot, 1 s current injections of increasing amplitude were delivered, and the average spike frequency during a step was determined by counting the number of spikes during the 1 s step and plotted against the injected current amplitude; calculations of the *F–I* plot based on the first instantaneous spike frequency gave equivalent results (data not shown). The slope of the *F–I* curve was linearly fitted. The voltage threshold for action potential generation was measured as the peak of the second derivative of voltage with time during the rising phase of the action potential. The spike afterhyperpolarization (AHP) amplitude was measured from the action potential threshold to the minimal voltage after the action potential. Additionally, we also measured the peak AHP, the minimal voltage after the action potential, with respect to ground. The spike amplitude was measured from the peak AHP to the peak of the action potential. The action potential half-width was established at the voltage halfway from the spike threshold to the peak of the action potential. The minimal amount of current necessary for spike generation was defined as rheobase in our measurements. The hyperpolarization-activated sag depolarization was determined with 1 s hyperpolarizing steps of increasing current amplitude to generate minimal voltages down to −128 mV. The sag voltage was measured from the minimal membrane potential near the beginning of the step to the voltage at the end of the step. During release of the hyperpolarizing steps, the neurons often rebounded with a small depolarization, which was measured relative to the holding potential (typically −68 mV). Input resistance was estimated by applying small hyperpolarizing current pulses. The effects of serotonin on the membrane properties were analyzed by paired two-tailed Student's *t* test. Results were considered statistically significant at $p < 0.05$. Data are expressed as mean ± SD.

Results

Identification of dCINs and adCINs in whole-cord preparations

To characterize the activity of dCINs and adCINs during fictive locomotion in neonatal mice, we performed whole-cell current-clamp recordings in whole-cord preparations during NMDA- and 5-HT-induced locomotor-like activity, characterized by left–right (iL2–cL2) and flexor–extensor (iL2–iL5) alternation in ventral root bursts (Fig. 1*B*). In P0–P3 mouse spinal cords, rhythmic locomotor-like behavior was reliably induced by 3–10 μM NMDA and 6–15 μM 5-HT; the step cycle period varied from 2 to 4 s (3.2 ± 0.9 s; $n = 43$). Cells were considered as commissural interneurons only if they passed a collision test (Fig. 1*C*) from contralateral hemicord stimulation with most fast synaptic transmission blocked by a combination of glutamatergic (10 μM CNQX and 15–20 μM AP-5), GABAergic (5 μM picrotoxin), and glycinergic (10 μM strychnine) receptor blockers. We differentiated dCINs from adCINs by stimulating both the rostral (T13–L1) and caudal (L4–L5) contralateral hemicords. dCINs passed the collision test with caudal but not rostral hemicord stimulation, whereas adCINs passed the collision test with both rostral and caudal hemicord stimulations (see example in Fig. 1*C*). During these experiments, we recorded from 210 neurons in the ventromedial area (laminas VII–VIII) from the L2 segment: 66 were identified as CINs, with 29 aCINs, 27 dCINs, and 10 adCINs.

Different firing patterns of dCINs and adCINs during NMDA- and 5-HT-induced locomotion

The firing patterns of dCINs during NMDA- and 5-HT-induced fictive locomotion and their monosynaptic and polysynaptic connections with contralateral motoneurons have already been investigated in neonatal rats: their firing patterns varied from highly rhythmic to nonrhythmic (Butt et al., 2002; Butt and Kiehn, 2003). However, this previous study did not discriminate dCINs from adCINs, because only a caudal hemicord stimulation was performed. Because we could distinguish these two neuron types by using two stimulation electrodes, we asked whether dCINs and adCINs have different firing patterns during fictive locomotion in the mouse.

We found that the firing pattern of identified dCINs was not homogeneous during fictive locomotion, ranging from tonic and nonrhythmic to highly rhythmic firing. In the example of Figure 2*A*, the dCIN fired highly rhythmically, with short bursts of action potentials at the transition from contralateral to ipsilateral ventral root bursting. When the phase of activity during a single cycle was calculated, this neuron showed a peak at the beginning of the ipsilateral L2 burst (Fig. 2*B*). We used circular statistics to determine the peak phase and rhythmicity of 16 dCINs (Fig. 2*C*). The majority of dCINs tested (13 of 16) fired rhythmically during fictive locomotion induced by 5-HT and NMDA (filled squares indicate significantly rhythmic firing with $p < 0.05$). As was seen previously with rat dCINs (Butt et al., 2002), the dCIN firing phase was widely distributed throughout the locomotor cycle, with peaks of activity during both the ipsilateral and contralateral flexor bursts (Fig. 2*C*). These neurons tended to fire in the second half of a ventral root burst: 9 of the 13 dCINs fired in either the second or fourth quadrant of the circular plot (Fig. 2*C*). Thus, dCINs in the neonatal mouse are not homogeneous in their firing phase during fictive locomotion.

In contrast, none of the adCINs we recorded during fictive locomotion ($n = 5$) showed significantly rhythmic firing activity. The neuron recorded in Figure 2*D* fired tonically before addition of NMDA and 5-HT, and this pattern was unchanged after fictive locomotion was initiated. There was no significant peak phase of activity during a cycle (Fig. 2*E*). Similar results were seen with four other adCINs (Fig. 2*F*).

Electrophysiological characterization of dCINs and adCINs

To determine whether the different locomotor-related firing patterns of dCINs and adCINs arise from different intrinsic membrane properties, we characterized these properties in the presence of blockers of rapid synaptic transmission (glutamate, GABA, and glycine) to reduce the effects of synaptic input on the neurons (Table 1). The resting membrane potentials of dCINs and adCINs were not significantly different (dCIN, −59.4 ± 5.6 mV, $n = 16$; adCIN, −57.1 ± 4.2 mV, $n = 8$; $p > 0.05$); the membrane capacitance of adCINs tended to

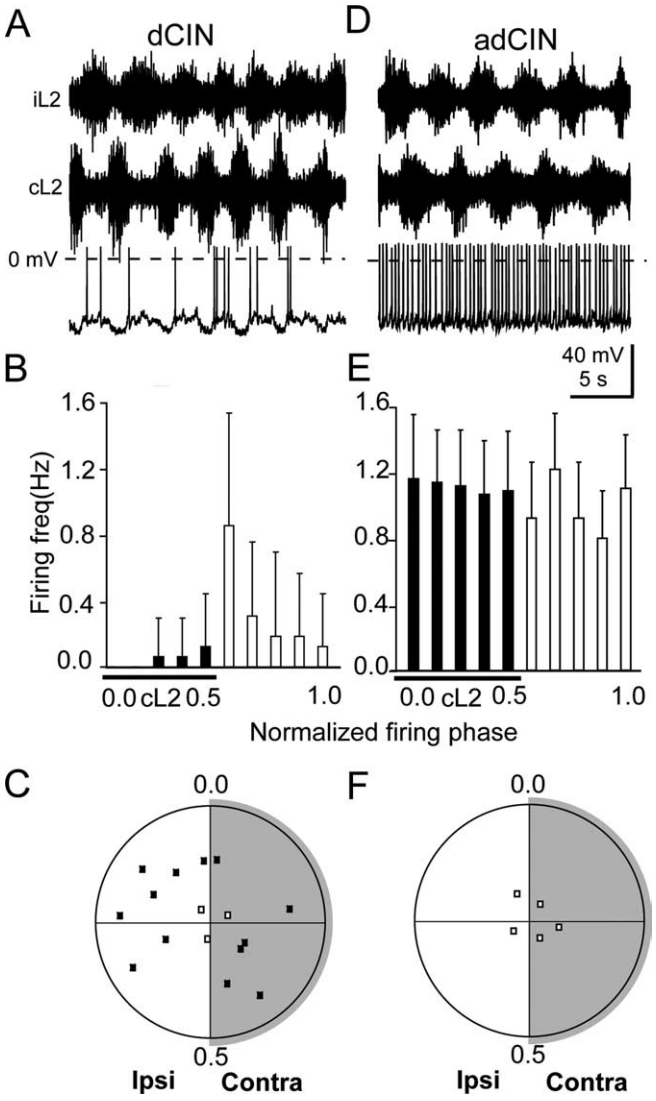

Figure 2. Firing pattern of dCINs and adCINs during fictive locomotion. ***A***, ***D***, Typical firing pattern of a dCIN and an adCIN during NMDA- and 5-HT-induced locomotor-like activity. ***B***, ***E***, Histogram of firing phase of the dCIN and the adCIN shown in ***A*** and ***D***. Average firing frequency in each time bin during the cycle is averaged over many cycles. ***C***, ***F***, Circular lots of the phase and rhythmicity of dCINs ($n = 16$) and adCINs ($n = 5$) derived from circular statistics. The direction of the vector represents the preferred phase of firing of the neuron, and the distance from the center indicates the statistical significance of the rhythmicity of the neuron. Filled squares are significantly rhythmic neurons ($p < 0.05$) (Zar, 2000), and open squares are not. Each small square represents the vector point for one experiment. Gray-shaded areas represent the contralateral L2 flexor phase.

be larger than dCINs but not significantly (Table 1). It should be noted that 3 of 19 dCINs and 1 of 9 adCINs displayed spontaneous tonic firing in the absence of bias current before NMDA and 5-HT application; the neurons did not differ in their average spike frequency under control conditions. To further investigate the membrane properties of the interneurons, their membrane potential before addition of serotonin was adjusted to −68 mV with bias current, and the membrane responses to a series of depolarizing and hyperpolarizing current steps were recorded. dCINs could be divided into two groups based on their firing responses to suprathreshold inputs (Fig. 3*A*). Most dCINs (20 of 27) displayed tonic firing throughout a suprathreshold depolarizing step (Fig. 3*A*, left and middle). However, seven dCINs fired only phasically and

Table 1. Comparison of the intrinsic membrane properties of aCINs, dCINs, and adCINs

	aCINs	dCINs	adCINs
E_m (mV)	−60.4 ± 3.6 (29)	−59.4 ± 5.6 (16)	−57.1 ± 4.2 (8)
R_{in} (M&OHgr;)	644.2 ± 276.4 (20)	571.4 ± 204.5 (11)	523.3 ± 191.5 (6)
C_m (pF)	70.2 ± 15.6 (30)	63.3 ± 10.4 (26)	75.1 ± 25.6 (9)
Rheobase (pA)	37.7 ± 22.8 (20)	33.5 ± 18.9 (11)	41.5 ± 29.1 (6)
AP amplitude (mV)	62.7 ± 8.5 (30)	61.8 ± 7.2 (27)	63.1 ± 9.5 (9)
AP half-width (ms)	3.0 ± 0.5 (30)	2.9 ± 0.6 (27)	3.1 ± 0.7 (9)
AP threshold (mV)	−40.0 ± 7.4 (30)	−39.4 ± 5.7 (27)	−37.8 ± 6.7 (9)
AHP amplitude (mV)	17.6 ± 3.2 (30)	16.2 ± 4.8 (27)	17.3 ± 4.5 (9)

AP, Action potential. Data for aCINs are from Zhong et al. (2006).

stopped firing before the step was ended (Fig. 3*A*, right). We further analyzed the properties of individual action potentials in these two dCIN groups. The spike threshold tended to be lower and the AHP amplitude tended to be smaller with phasic than tonic dCINs, but none of these comparisons were statistically significant (data not shown).

We then characterized the firing and membrane properties of adCINs. Almost all adCINs (9 of 10) displayed tonic firing during a step depolarization (Fig. 3*B*); the remaining adCIN fired only a single spike to any depolarizing step. This single spiking adCIN was not included in the later analysis. The action potential properties and other membrane properties of dCINs and adCINs are compared in Table 1. To allow full comparison, we also include in this table the corresponding data for aCINs (Zhong et al., 2006). Collectively, there were no significant differences between dCINs, aCINs, and adCINs for any of the parameters we measured.

We also measured the responses of the interneurons to hyperpolarizing current steps (Fig. 3). Most dCINs (22 of 27 neurons), including both tonic and phasic dCINs, displayed a prominent depolarizing voltage sag during a sustained hyper-

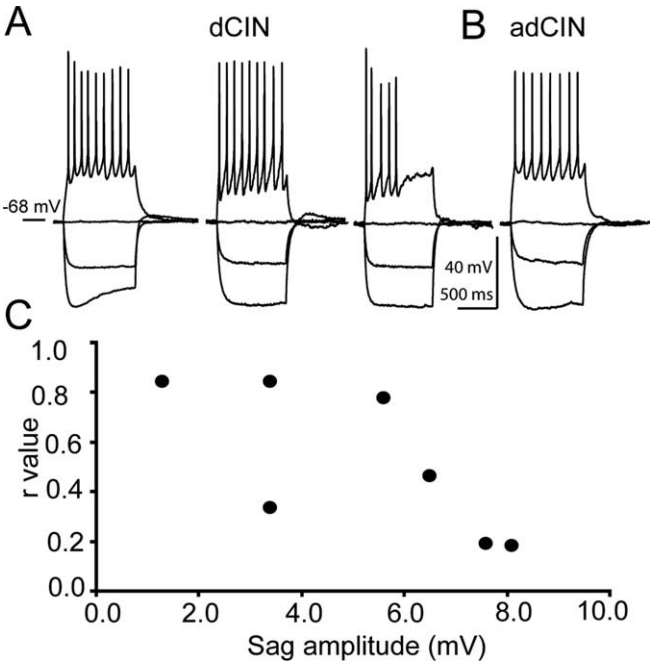

Figure 3. Electrophysiological properties of dCINs and adCINs and their distribution in neonatal mouse spinal cord. ***A***, The responses of three different dCINs to a series of current steps. ***B***, A typical response of an adCIN to different current steps. ***C***, The relationship between the sag amplitude and the rhythmicity of dCINs as determined by the *r* value in the circular statistics analysis.

polarizing step (Fig. 3*A*, left), which could be blocked by 2 mM Cs^+ or 100 μM ZD 7288 (4-ethylphenylamino-1,2-dimethyl-6-methylaminopyrimidinium chloride) (data not shown), suggesting that the depolarizing sag may be caused by a hyperpolarization-activated inward current. However, this was variable; some dCINs had a smaller sag potential (Fig. 3*A*, middle), and a few ($n = 5$) had no detectable sag at −128 mV (Fig. 3*A*, right). In contrast, the sag voltage in adCINs was much smaller than in dCINs. Quantitatively, the depolarizing sag, measured as the voltage difference between the minimum voltage and the voltage at the end of a 1 s hyperpolarizing step from −68 to −128 mV, was 7.4 ± 2.5 mV ($n = 21$) in dCINs but only 2.0 ± 0.7 mV($n = 9$) in adCINs ($p < 0.001$). Consistent with this result, the overshooting rebound potential after the end of the hyperpolarizing pulse was significantly larger in dCINs (3.8 ± 1.4 mV) than in adCINs (0.8 ± 0.4 mV; $p < 0.005$).

I_h does not appear to contribute to the rhythmicity of dCINs

The depolarizing sag likely arises from slow activation of the hyperpolarization-activated inward current, I_h, which is believed to play an important role in many rhythmic neurons from vertebrates and invertebrates (Angstadt and Calabrese, 1989; McCormick and Pape, 1990; Golowasch and Marder, 1992; Lüthi et al., 1998; Thoby-Brisson et al., 2000). The adCINs had a very small I_h and did not fire rhythmically during NMDA- and 5-HT-induced locomotor-like activity, whereas the dCINs had a larger sag voltage and did fire rhythmically. Thus, we tested whether this current contributes to the rhythmicity of dCINs by directly comparing the amplitude of the sag voltage with the rhythmicity of dCINs, determined by their *r* values from the circular statistics. As illustrated by Figure 3*C*, we did not find a positive correlation between the I_h sag amplitude and *r* value. dCINs that fired highly rhythmically could have either a very small or a large sag voltage, and the neurons firing nonrhythmically had the largest sag voltages. These results are consistent with those found in rat dCINs (Butt et al., 2002), suggesting that I_h does not contribute significantly to the rhythmicity of dCINs in the spinal cord from neonatal mice.

Effects of 5-HT on the membrane potential of dCINs and adCINs

5-HT plays an important role in enabling the generation of the locomotor rhythm in rodents (MacLean et al., 1998; Madriaga et al., 2004; Christie and Whelan, 2005; Liu and Jordan, 2005; Pearlstein et al., 2005). Thus, we examined the effects of 5-HT on the firing properties of dCINs and adCINs in the spinal cord of neonatal mice. To maintain all cells below threshold before application of 5-HT, the membrane potential was adjusted to −68 mV with bias current injection. The neurons were studied in the presence of blockers of fast glutamatergic, GABAergic, and glycinergic synaptic transmission to study the direct effects of serotonin on the cells. All dCINs ($n = 14$) were strongly depolarized by application of 9 μM 5-HT (Fig. 4*A*). In two cells, serotonin additionally evoked small (3.4 ± 0.4 mV) membrane oscillations that resembled truncated action potentials; these were seen more often in our previous study of aCINs, in which they were shown to arise from electrical coupling to unknown spiking neurons (Zhong et al., 2006). The depolarizing effect of 5-HT peaked at or shortly after the end of 5-HT application (Fig. 4*A*) and was fully reversible (data not shown). In contrast, 9 μM serotonin did not significantly alter the membrane potential of adCINs (Fig. 4*B*). On average, serotonin depolarized the dCINs by 7.7 ± 2.5 mV ($n = 14$; $p < 0.001$) but evoked a nonsignificant 1.9 ± 1.5 mV depolarization in adCINs ($n = 7$; $p > 0.05$).

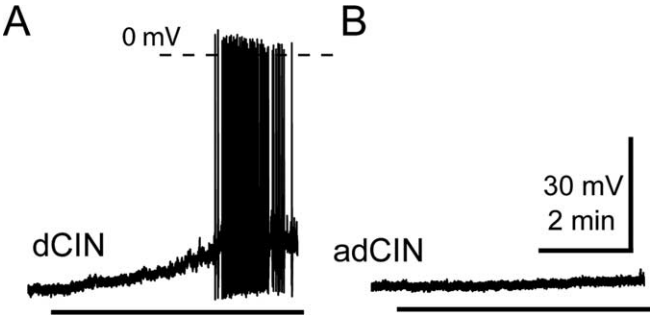

Figure 4. Effects of 5-HT on the membrane potential of dCINs and adCINs. ***A***, 5-HT (9 μM) depolarizes the membrane potential of a dCIN with most fast synaptic transmission blocked. ***B***, Effects of 5-HT (9 μM) on the membrane potential of an adCIN with most fast synaptic transmission blocked. The black bar indicates the application of 5-HT during Ringer's solution with AP-5 (20 μM), CNQX (10 μM), picrotoxin (5 μM), and strychnine (10 μM).

5-HT has little effect on input resistance, sag, and rebound potential in dCINs or adCINs

We next measured the effects of 5-HT on dCIN and adCIN voltage responses to a series of hyperpolarizing current steps (Fig. 5). The cell membrane potential was maintained by current injection at −68 mV during control, 5-HT, and washout conditions. 5-HT (9 μM) had no reproducible effect on the input resistance of dCINs (control, 571 ± 204 MΩ; 5-HT, 585 ± 245 MΩ; washout, 591 ± 230 MΩ; $n = 11$; $p > 0.1$) or adCINs (control, 510 ± 80 MΩ; 5-HT, 518 ± 91 MΩ; washout, 520 ± 89 MΩ; $n = 5$; $p > 0.2$). 5-HT also did not significantly alter the mean sag voltage evoked by hyperpolarizing current steps (Fig. 5). When measured after a step to a minimum potential of −128 mV, 5-HT did not alter the voltage sag in dCINs (control, 6.6 ± 4.6 mV; 5-HT, 6.1 ± 4.7 mV; washout, 5.9 ± 3.9 mV; $p > 0.2$; $n = 11$). adCINs had much smaller sag voltages, and these were also unaffected by 5-HT (control, 2.7 ± 1.5 mV; 5-HT, 2.5 ± 1.8 mV; washout, 2.2 ± 1.7 mV; $p > 0.1$; $n = 6$) (Fig. 5*B*). Finally, 5-HT did not increase the post-hyperpolarizing rebound potential in either dCINs (control, 4.1 ± 0.7 mV; 5-HT, 3.8 ± 0.9 mV; washout, 3.7 ± 0.8 mV; $p > 0.1$; $n = 11$) or adCINs (control, 0.8 ± 0.4 mV; 5-HT, 0.9 ± 0.4 mV; washout, 0.8 ± 0.3 mV; $p > 0.05$; $n = 6$).

Serotonin enhances the excitability of dCINs but not adCINs

The effects of 5-HT on the excitability of dCINs and adCINs were investigated in the presence of blockers of fast glutamatergic, GABAergic, and glycinergic synaptic transmission. Figure 6*A* shows the response of one dCIN to a 50 pA current step before, during, and after washout of serotonin application. Holding currents were adjusted to keep the membrane potential at −68 mV in the different conditions. The evoked spike frequency increased from 5 to 7 Hz by serotonin application. We quantified the responses of 11 dCINs to current steps that evoked 5 Hz firing responses under control conditions; in the presence of 5-HT, the firing frequency significantly increased (control, 4.7 ± 0.5 Hz; 5-HT, 7.1 ± 1.1 Hz; washout, 5.1 ± 1.2 Hz; $n = 11$; $p < 0.001$) (Fig. 6*A*, right). We generated *F–I* plots of the average spike frequency over a range of current step amplitudes; as found previously with aCINs (Zhong et al., 2006), serotonin caused a parallel upward shift in the frequency response to the current steps (Fig. 6*C*). Similar results

were observed in 10 other dCINs examined. As can be seen from the *F–I* plots, the rheobase value for spike generation was reduced by serotonin from 33.5 ± 18.9 to 21.5 ± 15.6 pA ($p < 0.001$).

In contrast, 5-HT did not significantly alter the excitability of adCINs. The response of one adCIN to a 60 pA depolarizing step during control, 5-HT, and washout conditions is shown in Figure 6*B*. Serotonin did not increase the firing frequency or alter the firing pattern. Similar findings were observed in five other adCINs in which, under control conditions, the neurons fired at 5.1 ± 1.2 Hz; 5-HT did not change this (5.2 ± 1.4 Hz), and there was no significant change during washout (4.9 ± 1.5 Hz; $n = 5$; $p > 0.2$). The *F–I* relationship in adCINs was also unaffected by serotonin: one example is given in Figure 6*D*, and similar results were seen in five other adCINs. These results show that 5-HT depolarizes and enhances the excitability of dCINs just as they do aCINs (Zhong et al., 2006) but has no significant effect on adCINs.

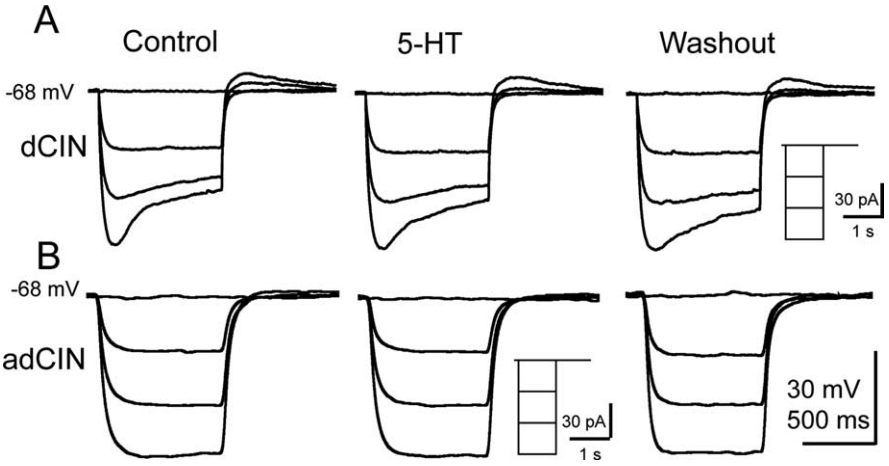

Figure 5. Effects of 5-HT on the dCIN and adCIN responses to hyperpolarizing current steps. ***A***, dCIN response to increasing hyperpolarizing 1 s current pulses during control, 5-HT (9 μM), and washout conditions with most fast synaptic transmission blocked. The small trace is the stimulation protocol. ***B***, adCIN response to increasing hyperpolarizing current pulses during control, 5-HT (9 μM), and washout conditions with most fast synaptic transmission blocked. The small trace is the stimulation protocol.

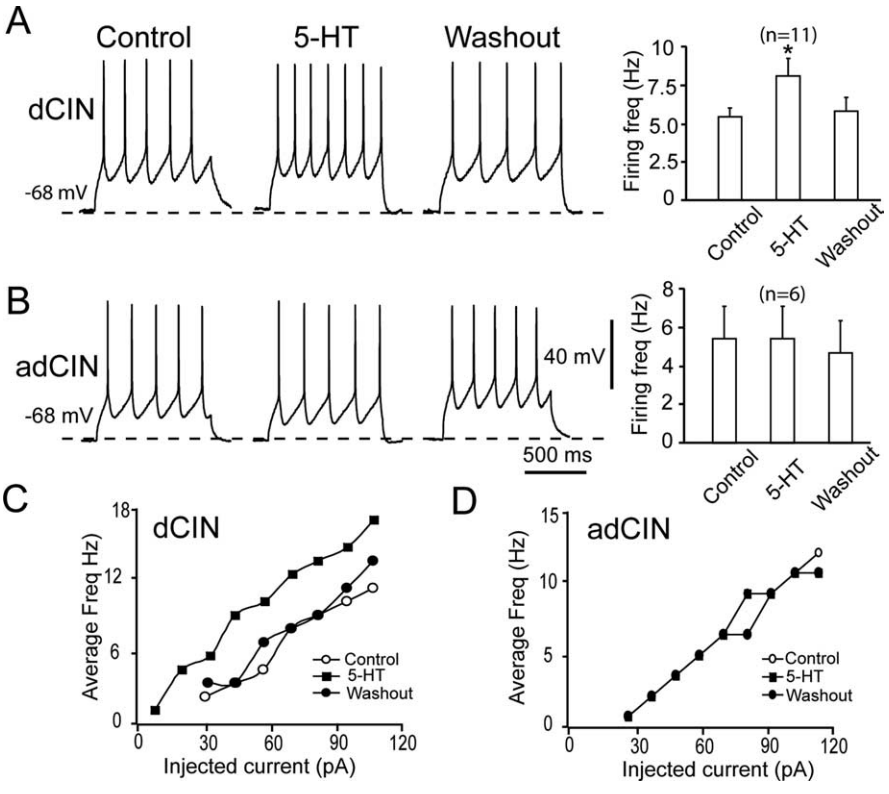

Figure 6. Effects of 5-HT on the excitability of dCINs and adCINs. ***A***, Left, Responses of a dCIN to a constant 50 pA depolarizing current step during control, 5-HT (9 μM), and washout conditions with most fast synaptic transmission blocked. Right, Average effects of 5-HT on excitability of 11 dCINs. *$p < 0.05$. ***B***, Left, Responses of an adCIN to a depolarizing current step during control, 5-HT (9 μM), and washout conditions with most fast synaptic transmission blocked. Right, Effects of 5-HT on excitability of six adCINs. ***C***, ***D***, Effects of 5-HT on the *F–I* relationship in a dCIN and an adCIN, respectively.

Effects of 5-HT on AHP and spike threshold

The voltage threshold for action potential generation evoked by minimal current injection from a membrane potential of −68 mV was measured as the peak of the second derivative of voltage with time during the rising phase of the action potential. As expected from the reduced rheobase in serotonin, the amine decreased the action potential threshold in dCINs significantly (control, −38.2 ± 4.3 mV; 5-HT, −41.2 ± 4.0 mV; washout, −39.3 ± 4.2 mV; $n = 11$; $p < 0.001$) (Fig. 7*A*,*C*). The postspike AHP affects neuronal excitability and maximum spike frequency (Wallen et al., 1989). We found that serotonin also significantly reduced the amplitude of the AHP (relative to the spike threshold) by 20% (control, 16.1 ± 3.7 mV; 5-HT, 12.7 ± 3.1 mV; washout, 14.4 ± 3.5 mV; $n = 11$; $p < 0.001$) (Fig. 7*B*,*D*). This is a real reduction in AHP amplitude, because the absolute value of the AHP (relative to 0 mV) was also reduced from −56.4 ± 4.2 to −54.5 ± 5.3 mV ($p < 0.001$; $n = 11$). Unlike the aCINs (Zhong et al., 2006), 5-HT had no significant effects on the half-width or amplitude of the action potential in the dCINs. We also characterized the effects of 5-HT on adCIN action potentials. None of the action potential parameters were changed by application of 5-HT, including spike threshold, AHP amplitude, half-width, and spike amplitude (data not shown). Thus, 5-HT differently affected the action potential properties of dCINs and aCINs (Zhong et al., 2006) but not adCINs from L2 segment in the neonatal mouse spinal cord.

Discussion

Distinct subpopulations of CINs in the neonatal mouse spinal cord

We studied the properties of two distinct subsets of CINs located in the ventromedial area of the lumbar spinal cord (L2). When the cord is split longitudinally, each hemicord can generate its own locomotor rhythm, suggesting that CINs are not essential for rhythmogenesis (Bonnot and Morin, 1998; Branchereau et al.,

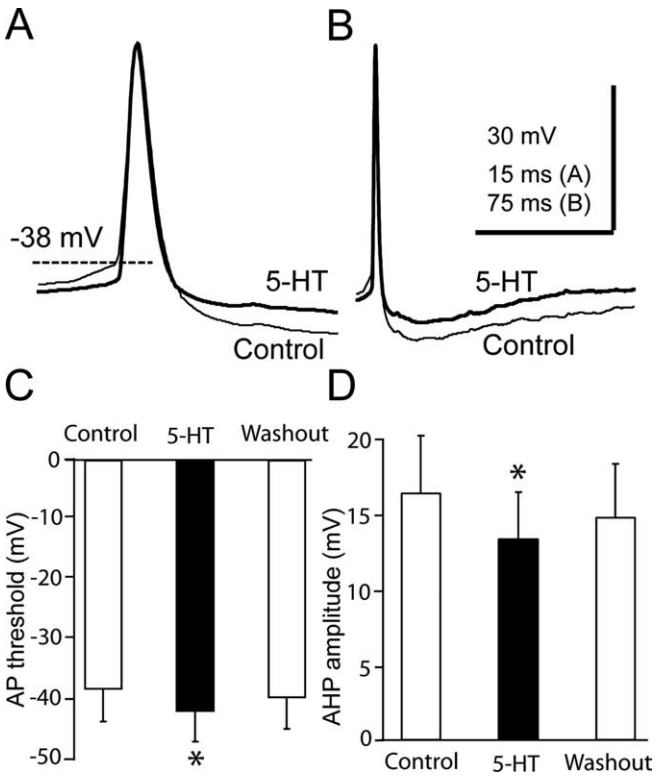

Figure 7. Effects of 5-HT on the individual action potential properties in dCINs. ***A***, Changes in spike threshold of a dCIN during control and 5-HT conditions. ***B***, Same neuron as ***A***, at a slower timescale, showing a reduction of the afterhyperpolarization amplitude with 5-HT. For clarity, the washout traces are not shown in ***A*** and ***B***. ***C***, Average effects of 5-HT on action potential threshold ($n = 11$). ***D***, Average effects of 5-HT on AHP amplitude ($n = 11$). $^*p < 0.05$.

2000). In the intact cord, CINs coordinate these independent oscillators to generate left–right alternation in many species, including lamprey (Buchanan and McPherson, 1995; Buchanan, 1999), *Xenopus* tadpoles (Soffe et al., 1984), cats (Matsuyama et al., 2004), and fetal (Nakayama et al., 2002) and neonatal (Butt et al., 2002; Butt and Kiehn, 2003) rats. In cats and neonatal rodents, CINs are heterogeneous in their effects: glutamatergic and glycinergic CINs provide contralateral excitation and inhibition, respectively, to motoneurons and interneurons at different phases of the fictive motor pattern (Bannatyne et al., 2003; Birinyi et al., 2003; Butt and Kiehn, 2003; Butt et al., 2003).

Our results explore the activity of dCINs and adCINs during locomotion in the neonatal mouse. As seen previously in the neonatal rat (Butt et al., 2002), during fictive locomotion in neonatal mice, 81% of the dCINs fired rhythmically, with peaks of activity over a wide range of the cycle. dCINs have similar firing patterns to aCINs (Zhong et al., 2006), suggesting that both aCINs and dCINs could be involved in coordinating left–right alternation. Different dCINs fire rhythmically with the ipsilateral or contralateral flexor phase; most of the dCINs fired in the second half of a ventral root burst, and some fired specifically during the transition between left and right bursts (Fig. 2). This suggests that these interneurons may be involved in initiating the switch in activity to the opposite side. The central pattern generator (CPG) for locomotion is distributed over a number of spinal segments from the lower thoracic to the lower lumbar spinal cord, and both flexor- and extensor-related interneuron activity is present in many segments (Cazalets et al., 1995; Kjaerulff and Kiehn, 1996; Cowley and Schmidt, 1997; Kremer and Lev-Tov, 1997; Kiehn and Kjaerulff, 1998). Thus, CINs extending axons both rostrally and caudally from their segments of origin would help in coordinating the activity of this highly distributed network.

In contrast, adCINs, which send their axons in both rostral and caudal directions, did not fire rhythmically during fictive locomotion, suggesting that they do not participate in the locomotor CPG under these conditions. However, because these interneurons were rarely found, it is possible that we did not record from all the types of adCINs. These interneurons could play important roles in nonrhythmic spinal functions such as reflexes, which are still important during locomotion.

We also studied the intrinsic membrane properties of dCINs and adCINs in the absence of most rapid synaptic inputs. The dCINs show heterogeneous responses to a step depolarization, with some firing tonically whereas other phasic neurons fire only a short burst before falling silent. Both tonic and phasic populations can fire rhythmically during fictive locomotion. Almost all adCINs display a tonic firing pattern to suprathreshold inputs. Membrane responses to hyperpolarizing inputs also showed a difference between the two cell types: none of the adCINs showed a strong depolarizing sag at −128 mV, whereas most of the tonic and phasic firing dCINs did. This raised the possibility that I_h could contribute to the rhythmic firing of dCINs during fictive locomotion. This possibility is unlikely because the rhythmicity of dCINs was not correlated with the amplitude of the sag (Fig. 3*C*); a similar conclusion was drawn for I_h in dCINs in the rat spinal cord (Butt et al., 2002). However, our experimental results do not exclude the possibility of a role for I_h in other interneurons during NMDA/5-HT-induced locomotor-like activity. Overall, our results support the hypothesis that both tonic and phasic dCINs, as well as aCINs (Zhong et al., 2006), are likely to participate in left–right coordination of the locomotor rhythm in neonatal mice, but adCINs are not.

Different modulation of dCINs and adCINs by serotonin

Serotonin is important for rhythm generation in lamprey (Zhang and Grillner, 2000) and helps to shape the development of locomotion in zebrafish (Brustein et al., 2003) and *Xenopus* tadpoles (McLean et al., 2000). Serotonin also plays a central role in enabling the CPG for locomotion in the neonatal rodent (MacLean et al., 1998; Madriaga et al., 2004; Christie and Whelan, 2005; Liu and Jordan, 2005; Pearlstein et al., 2005). 5-HT receptor antagonists can abolish NMDA-evoked fictive locomotion in the rat (MacLean et al., 1998), and both ketanserin (a 5-HT_2 receptor antagonist) and SB 269970 [(*R*)-3-(2-(2-(4-methylpiperidin-1-yl)-ethyl)pyrrolidine-1-sulfonyl)phenol] (a 5-HT_7 receptor antagonist) disrupt the locomotor-like activity induced by electrical stimulation from brainstem in neonatal rodent spinal cord (Liu and Jordan, 2005; Pearlstein et al., 2005). Because the hemicord is sufficient to generate a locomotor-like rhythm (Bonnot and Morin, 1998; Branchereau et al., 2000), it was not obvious that 5-HT would also affect the CINs, which could in theory be unaffected by the amine and passively transfer the information between the two sides of the cord.

Our intracellular recordings show that, in the neonatal mouse, 5-HT probably depolarizes and excites the dCINs directly, because rapid glutamatergic, GABAergic, and glycinergic synaptic transmissions are blocked in our recordings. However, we cannot eliminate the possibility that 5-HT exerts its effects in part presynaptically, because ascending CINs have been shown recently to be excited by acetylcholine (Carlin et al., 2006), which we did not block. These neurons are also probably modulated by other metabotropic inputs [for example, metabotropic glutamatergic inputs (Taccola et al., 2003, 2004)], although they have not yet

been identified. In addition, in a few dCINs with most fast synaptic transmission blocked, serotonin evoked small oscillations resembling truncated action potentials; these were seen previously in aCINs (Zhong et al., 2006) in which we showed that they arise from electrical coupling to unidentified neurons. Supporting a direct effect on the CINs, 5-HT modified the action potential properties in dCINs, decreasing the voltage threshold for action potential generation. This is in agreement with previous studies in rat motoneurons and unidentified ventral horn neurons, in which 5-HT reduces the threshold for the action potential generation, making neurons more excitable to synaptic inputs (Fedirchuk and Dai, 2004; Gilmore and Fedirchuk, 2004). We also showed that the amplitude of the postspike AHP is reduced in dCINs; this can contribute to neuronal excitability (Grillner, 2003). Collectively, these effects of 5-HT all contribute to the increase of dCIN excitability in the neonatal mouse spinal cord. However, we do not yet have enough information to explain the ionic mechanisms underlying excitatory actions of 5-HT. The depolarization combined with a reduction in spike threshold could certainly contribute to the reduction in rheobase for spike initiation. Reduction in AHP amplitude has been associated with an increase in the *F–I* relationship, but this is usually accompanied by an increase in the slope of the relationship (Sourdet et al., 2003; Perez-Rosello et al., 2005), which we did not observe. This suggests that 5-HT excitation involves more than a simple reduction of the calcium-activated potassium current underlying the AHP, perhaps by the addition of a tonic or persistent inward current. Our results suggest that, in these neurons, I_h is not a major target of serotonin action, because the hyperpolarization-activated sag voltage was unaffected by 5-HT. Voltage-clamp studies of 5-HT effects on identified ionic currents will resolve these questions.

In contrast, 5-HT had no significant effects on the adCINs. It did not affect the basic membrane or action potential properties of these neurons and had no effect on either their membrane potential or excitability. Because adCINs are relatively rare in the lumbar ventromedial spinal cord (Stokke et al., 2002; Nissen et al., 2005) and thus hard to find, we cannot eliminate the possibility that other types of adCINs exist. It might be more feasible to investigate this problem in spinal cord slices in which the neurons can be visualized by double axonal prelabeling techniques (Eide et al., 1999; Stokke et al., 2002).

In summary, our results, in combination with our previous study of the aCINs (Zhong et al., 2006), show that the large majority of aCINs and dCINs are directly excited by serotonin, which enables the locomotor pattern generator in the neonatal rodent spinal cord, and fire rhythmically during NMDA- and 5-HT-induced locomotor-like activity. In contrast, adCINs are unaffected by serotonin and do not fire rhythmically during NMDA- and 5-HT-induced locomotor-like activity. Our results suggest that aCINs and dCINs, but not adCINs, are likely components of the hindlimb CPG, helping to organize left–right coordination during fictive locomotion in the neonatal mouse spinal cord. Because serotonin plays a critical role in enabling the rodent locomotor CPG, it is reassuring that neurons, which may be involved in the CPG, are directly affected by the amine. However, this is not a necessary condition because, in simpler invertebrate CPG networks, a neuromodulator can activate or modify the motor pattern by selected actions on a subset of the CPG neurons (Flamm and Harris-Warrick, 1986a,b; Harris-Warrick and Marder, 1991; Swensen and Marder, 2000, 2001). Our results, combined with that of others (Butt et al., 2002; Butt and Kiehn, 2003, Carlin et al., 2006, Zhong et al., 2006), shows the importance of classifying the interneuron populations that participate in the locomotor CPG; even very similar interneurons can have very different actions within the network.

References

Angstadt JD, Calabrese RL (1989) A hyperpolarization-activated inward current in heart interneurons of the medicinal leech. J Neurosci 9:2846–2857.

Bannatyne BA, Edgley SA, Hammar I, Jankowska E, Maxwell DJ (2003) Networks of inhibitory and excitatory commissural interneurons mediating crossed reticulospinal actions. Eur J Neurosci 18:2273–2284.

Berkowitz A, Stein PSG (1994) Activity of descending propriospinal axons in the turtle hindlimb enlargement during two forms of fictive scratching: phase analyses. J Neurosci 14:5105–5119.

Birinyi A, Viszokay K, Weber I, Kiehn O, Antal M (2003) Synaptic targets of commissural interneurons in the lumbar spinal cord of neonatal rats. J Comp Neurol 461:429–440.

Bonnot A, Morin D (1998) Hemisegmental localisation of rhythmic networks in the lumbosacral spinal cord of neonate mouse. Brain Res 793:136–148.

Branchereau P, Morin D, Bonnot A, Ballion B, Chapron J, Viala D (2000) Development of lumbar rhythmic networks: from embryonic to neonate locomotor-like patterns in the mouse. Brain Res Bull 53: 711–718.

Brustein E, Chong M, Holmqvist B, Drapeau P (2003) Serotonin patterns locomotor network activity in the developing zebrafish by modulating quiescent periods. J Neurobiol 57:303–322.

Buchanan JT (1999) Commissural interneurons in rhythmic generation and intersegmental coupling in the lamprey spinal cord. J Neurophysiol 81:2037–2045.

Buchanan JT, McPherson DR (1995) The neuronal network for locomotion in the lamprey spinal cord: evidence for the involvement of commissural interneurons. J Physiol (Paris) 89:221–234.

Butt SJ, Kiehn O (2003) Functional identification of interneurons responsible for left-right coordination of hindlimbs in mammals. Neuron 38:953–963.

Butt SJ, Harris-Warrick RM, Kiehn O (2002) Firing properties of identified interneuron population in the mammalian hindlimb central pattern generator. J Neurosci 22:9961–9971.

Carlin KP, Dai Y, Jordan LM (2006) Cholinergic and serotonergic excitation of ascending commissural neurons in the thoraco-lumbar spinal cord of the neonatal mouse. J Neurophysiol 95:1278–1284.

Cazalets JR, Squalli-Houssaini Y, Clarac F (1992) Activation of the central pattern generators for locomotion by serotonin and excitatory amino acids in neonatal rat. J Physiol (Lond) 455:187–204.

Cazalets JR, Borde M, Clarac F (1995) Localization and organization of the central pattern generator for hindlimb locomotion in newborn rat. J Neurosci 15:4943–4951.

Christie KJ, Whelan PJ (2005) Monoaminergic establishment of rostrocaudal gradients of rhythmicity in the neonatal mouse spinal cord. J Neurophysiol 94:1554–1564.

Cowley KC, Schmidt BJ (1997) Regional distribution of the locomotor pattern-generating network in the neonatal rat spinal cord. J Neurophysiol 77:247–259.

Eide AL, Glover J, Kjaerulff O, Kiehn O (1999) Characterization of commissural interneurons in the lumbar region of the neonatal rat spinal cord. J Comp Neurol 403:332–345.

Fedirchuk B, Dai Y (2004) Monoamines increase the excitability of spinal neurones in the neonatal rat by hyperpolarizing the threshold for action potential production. J Physiol (Lond) 557:355–361.

Flamm RE, Harris-Warrick RM (1986a) Aminergic modulation in lobster stomatogastric ganglion. I. Effects on motor pattern and activity of neurons within the pyloric circuit. J Neurophysiol 55:847–865.

Flamm RE, Harris-Warrick RM (1986b) Aminergic modulation in lobster stomatogastric ganglion. II. Target neurons of dopamine, octopamine, and serotonin within the pyloric circuit. J Neurophysiol 55:866–881.

Gilmore J, Fedirchuk B (2004) The excitability of lumbar motoneurones in the neonatal rat is increased by a hyperpolarization of their voltage threshold for activation by descending serotonergic fibres. J Physiol (Lond) 558:213–224.

Golowasch J, Marder E (1992) Ionic current of the lateral pyloric neuron of the stomatogastric ganglion of the crab. J Neurophysiol 67:318–331.

Grillner S (2003) The motor infrastructure: from ion channels to neuronal networks. Nat Rev Neurosci 4:573–586.

Harris-Warrick RM, Marder E (1991) Modulation of neural networks for behavior. Annu Rev Neurosci 14:39–57.

Kiehn O, Kjaerulff O (1998) Distribution of central pattern generators for rhythmic motor outputs in the spinal cord of limbed vertebrates. Ann NY Acad Sci 860:110–129.

Kjaerulff O, Kiehn O (1996) Distribution of networks generating and coordinating locomotor activity in the neonatal rat spinal cord *in vitro*: a lesion study. J Neurosci 16:5777–5794.

Kremer E, Lev-Tov A (1997) Localization of the spinal network associated with generation of hindlimb locomotion in the neonatal rat and organization of its transverse coupling system. J Neurophysiol 77:1155–1170.

Lanuza GM, Gosgnach S, Pierani A, Jessell TM, Goulding M (2004) Genetic identification of spinal interneurons that coordinate left-right locomotor activity necessary for walking movements. Neuron 42:375–386.

Liu J, Jordan LM (2005) Stimulation of the parapyramidal region of the neonatal rat brain stem produces locomotor-like activity involving spinal 5-HT7 and 5-HT2A receptors. J Neurophysiol 94:1392–1404.

Lüthi A, Bal T, McCormick DA (1998) Periodicity of thalamic spindle waves is abolished by ZD 7288, a blocker of I_h. J Neurophysiol 79:3284–3289.

MacLean JN, Cowley KC, Schmidt BJ (1998) NMDA receptor-mediated oscillatory activity in the neonatal rat spinal cord is serotonin dependent. J Neurophysiol 79:2804–2808.

Madriaga MA, McPhee LC, Chersa T, Christie KJ, Whelan PJ (2004) Modulation of locomotor activity by multiple 5-HT and dopaminergic receptor subtypes in the neonatal mouse spinal cord. J Neurophysiol 92:1566–1576.

Matsuyama K, Nakajima K, Mori F, Aoki M, Mori S (2004) Lumbar commissural interneurons with reticulospinal inputs in the cat: morphology and discharge patterns during fictive locomotion. J Comp Neurol 474:546–561.

McCormick DA, Pape HC (1990) Properties of a hyperpolarization-activated cation current and its role in rhythmic oscillation in thalamic relay neurons. J Physiol (Lond) 431:291–318.

McLean DL, Merrywest SD, Sillar KT (2000) The development of neuromodulatory systems and the maturation of motor patterns in amphibian tadpoles. Brain Res Bull 53:595–603.

Nakayama K, Nishimaru H, Kudo N (2002) Basis of changes in left-right coordination of rhythmic motor activity during development in the rat spinal cord. J Neurosci 22:10388–10398.

Nissen UV, Mochida H, Glover JC (2005) Development of projection-specific interneurons and projection neurons in the embryonic mouse and rat spinal cord. J Comp Neurol 483:30–47.

Pearlstein E, Ben Mabrouk F, Pflieger JF, Vinay L (2005) Serotonin refines the locomotor related alternations in the in vitro neonatal rat spinal cord. Eur J Neurosci 21:1338–1346.

Perez-Rosello T, Figueroa A, Salgado H, Vilchis C, Tecuapetla F, Guzman JN, Galarraga E, Bargas J (2005) Cholinergic control of firing pattern and neurotransmission in rat neostriatal projection neurons: role of CaV2.1 and CaV2.2 Ca^{2+} channels. J Neurophysiol 93:2507–2519.

Quinlan KA, Kiehn O (2005) Synaptic effects of intrasegmental commissural interneurons in the mouse spinal cord. Soc Neurosci Abstr 31:516.1.

Shefchyk SJ, Jordan LM (1985) Motoneuron input-resistance changes during fictive locomotion produced by stimulation of the mesencephalic locomotor region. J Neurophysiol 54:1101–1108.

Soffe SR, Clarke JD, Roberts A (1984) Activity of commissural interneurons in spinal cord of *Xenopus* embryos. J Neurophysiol 51:1257–1267.

Sourdet V, Russier M, Daoudal G, Ankri N, Debanne D (2003) Long-term enhancement of neuronal excitability and temporal fidelity mediated by metabotropic glutamate receptor subtype 5. J Neurosci 23:10238–10248.

Stokke MF, Nissen UV, Glover JC, Kiehn O (2002) Projection patterns of commissural interneurons in the lumbar spinal cord of the neonatal rat. J Comp Neurol 446:349–359.

Swensen AM, Marder E (2000) Multiple peptides converge to activate the same voltage-dependent current in a central pattern-generating circuit. J Neurosci 20:6752–6759.

Swensen AM, Marder E (2001) Modulators with convergent cellular actions elicit distinct circuit outputs. J Neurosci 21:4050–4058.

Taccola G, Marchetti C, Nistri A (2003) Effect of metabotropic glutamate receptor activity on rhythmic discharges of the neonatal rat spinal cord in vitro. Exp Brain Res 153:388–393.

Taccola G, Marchetti C, Nistri A (2004) Modulation of rhythmic patterns and cumulative depolarization by group I metabotropic glutamate receptors in the neonatal rat spinal cord in vitro. Eur J Neurosci 19:533–541.

Thoby-Brisson M, Telgkamp P, Ramirez JM (2000) The role of the hyperpolarization-activated current in modulating rhythmic activity in the isolated respiratory network of mice. J Neurosci 20:2994–3005.

Wallen P, Buchanan JT, Grillner S, Hill RH, Christenson J, Hokfelt T (1989) Effects of 5-hydroxytryptamine on the afterhyperpolarization, spike frequency regulation, and oscillatory membrane properties in lamprey spinal cord neurons. J Neurophysiol 61:759–768.

Zar JH (2000) Biostatistical analysis. Englewood Cliffs, NJ: Prentice-Hall.

Zhang W, Grillner S (2000) The spinal 5-HT system contributes to the generation of fictive locomotion in lamprey. Brain Res 879:188–192.

Zhong G, Diaz-Rios M, Harris-Warrick RM (2006) Serotonin modulates the properties of ascending commissural interneurons in the neonatal mouse spinal cord. J Neurophysiol 95:1545–1555.